Improving biochar properties by co-pyrolysis of pig manure with bio-invasive weed for use as the soil amendment

Jing Qiu[1*], Marcella Fernandes de Souza[1], Ana A. Robles-Aguilar[1], Stef Ghysels[2], Yong Sik Ok[3], Frederik Ronsse[2], Erik Meers[1]

[1] Department of Green Chemistry and Technology, Faculty of Bioscience Engineering, Ghent University, Coupure links 653, 9000 Ghent, Belgium

[2] Thermochemical Conversion of Biomass Research Group, Department of Green Chemistry and Technology, Ghent University, Coupure Links 653, 9000 Ghent, Belgium

[3] Korea Biochar Research Center, APRU Sustainable Waste Management Program & Division of Environmental Science and Ecological Engineering, Korea University, Seoul 02841, Republic of Korea

***Corresponding Author:**

Email: Qiu.Jing@UGent.be

Tel: +32(0)465105856

Address: Department of Green Chemistry and Technology, Faculty of Bioscience Engineering, Ghent University, Coupure links 653, 9000 Ghent, Belgium

Abstract

Over recent years, pyrolysis has grown into a mature technology with added value for producing soil improvers. Further innovations of this technology lie in developing tailor-made products from specific feedstocks (or mixtures thereof) in combination with adjusted mixing ratio-temperature regimes. In this context, co-pyrolysis of pig manure (PM) and the invasive plant Japanese knotweed (JK) at different mixture ratios (w/w) of 3:1 (P3J1), 1:1 (P1J1), and 1:3 (P1J3) and varying temperatures (400-700 °C) was studied to address the low carbon properties and heavy metals (HMs) risks of manure-derive biochars and beneficially ameliorate the bio-invasion situation by creating value from the plant biomass. Co-pyrolysis of PM with JK increased by nearly 1.5 folds the fixed carbon contents in the combined feedstock biochars obtained at 600 °C compared with PM-derived biochar alone, and all combined feedstock biochars met the requirements for soil improvement and carbon sequestration. The total HMs in PM biochars were significantly reduced by adding JK. The combined feedstock biochar P1J1 generated at 600 °C was the most effective in transforming Cu and Zn into more stable forms, accordingly reducing the associated environmental risk of heavy metal leaching from the biochar. In addition, the accumulation of macronutrients can be an added benefit of the co-pyrolysis process, and P1J1-600 was also the biochar that retained the most nutrients (P, Ca, Mg, and K).

Keywords: Pig manure, Invasive plant, Biochar aromaticity, Metal speciation, Nutrients

41 **Graphical Abstract**

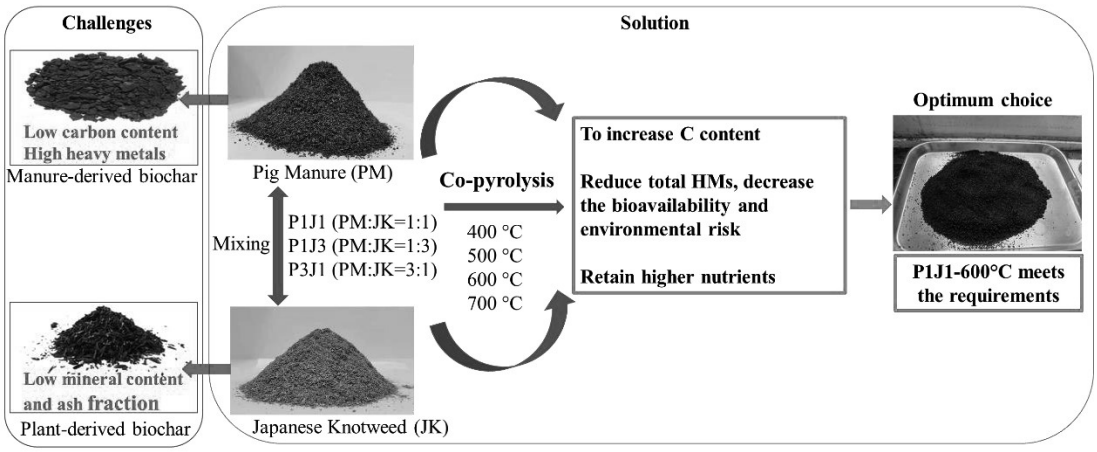

42

Highlights

- Japanese knotweed addition improved the aromaticity of pig manure-derived biochar
- Co-pyrolysis reduced total Cu and Zn compared to pig manure-derived biochar
- Cu and Zn transformed to stable forms reduce the environmental risk of the biochar
- Co-pyrolysis retained higher nutrients than Japanese knotweed-derived biochar alone
- A 1:1 ratio of pig manure to Japanese knotweed at 600°C was the optimal condition

1. Introduction

Turning animal manures into biochar via pyrolysis has received widespread attention recently (Garlapalli et al., 2016; Ghysels et al., 2020). This thermochemical conversion technology can minimize the volume of manure, kill pathogens and parasites and, more importantly, convert manure into high-performance bio-energy carriers (bio-oil and pyrolytic gas) and a carbon-rich solid (biochar) (Kameyama et al., 2020). Manure-derived biochar exhibits high pH, a favorable porous structure, is rich in ash and minerals and has various functional groups. It also has been reported to be an effective amendment to enhance the physicochemical and biological properties of soil, improve fertility, immobilize heavy metals for soil remediation (Mendonça et al., 2017), and reduce GHGs by carbon sequestration (Jiang et al., 2018; Li et al., 2020).

However, some limitations of manure-derived biochar, including low C content and the significant presence of heavy metals (like Cu and Zn), bring a critical level of uncertainty to the feasibility of using this product as a soil improver (Xu et al., 2019). Plant-based biochar, on the contrary, has been reported to have characteristics of high aromaticity, high C contents, and low heavy metal content (Xing et al., 2021). Therefore, co-pyrolysis of manure with plants might compensate for the shortcomings of the manure-derived biochar by diluting the heavy metals and increasing the final carbon content. Moreover, plant-derived biochar generally contains a low mineral content and a reduced ash fraction (Gao et al., 2020), characteristics associated with reduced nutrient content and heavy metal retention capacity (Xing et al., 2021). It, therefore, could also benefit from co-pyrolysis with manure to overcome these limitations.

Co-pyrolysis has been extensively explored for the joint pyrolysis of manure with agricultural

71 wastes to reduce the total and available metal of manure-derived biochar (Xu et al., 2019); still,
72 some inconsistent results regarding stabilization or mobilization of heavy metals have been
73 reported (Huang et al., 2017; Meng et al., 2018). Additionally, while previous works have
74 investigated the aromaticity (carbon) and agricultural benefits (nutrients) of manure-derived
75 co-pyrolysis biochar (Zhang et al., 2020), most studies focus either on heavy metals, carbon,
76 nutrients, or a combination of two parameters (Rodriguez et al., 2021). Co-pyrolysis of manure
77 with plants as a strategy to repress both disadvantages of plant-derived biochar and manure-
78 derived biochar has not been fully considered in a systematic evaluation of the final combined
79 feedstock biochar for its potential use as an optimum soil amendment. Moreover, the
80 characteristics of co-pyrolyzed biochar are determined by feedstock types, pyrolysis
81 temperatures, residence times, and mixture ratios (Ahmed and Hameed, 2020); thus, to confirm
82 the contributions of each material and the potential ecological and agronomic applications,
83 more studies are needed to verify the performance of co-pyrolyzed biochar from manure and
84 plant biomass covering different blending ratios and pyrolysis temperatures.

85 The most invasive weed in Belgium is *Fallopia japonica*, commonly known as Japanese
86 knotweed, originally from East Asia and currently invading much of Europe, dislodging native
87 plants from disturbed habitats and damaging the local ecological system (Alfieri and Mann,
88 2015). Converting invasive plant biomass to biochar through pyrolysis controls the expansion
89 of exotic plants and efficiently uses this waste to achieve ecological and economic benefits
90 (Feng et al., 2021). Pig farming in the EU is concentrated in certain areas, with about 30% of
91 the animals located in a major pig production basin that stretches from Denmark through
92 northwestern Germany and the Netherlands to northern Belgium (Makara and Kowalski, 2018),

93 which results in a pig manure abundance of over 120 million tons per year (Köninger et al.,
94 2021). Consequently, Japanese knotweed and pig manure were selected in this study due to
95 their large amount and the need for proper disposal in Belgium.

96 Co-pyrolysis of pig manure and Japanese knotweed for biochar production can achieve a "triple
97 win" of safely treating manure, disposing of the invasive plant, and producing high-quality
98 biochar. The aims of this study were, therefore, 1) to assess the effects in co-pyrolysis of pig
99 manure with Japanese knotweed on biochar carbon properties; 2) to determine the levels of
100 HMs in the produced biochars and their bioavailability; 3) to explore the environmental risks
101 associated with HMs in biochars, and 4) to predict the nutrients retention value of generated
102 biochars. To achieve these, mixtures of pig manure and Japanese knotweed were treated at
103 different mass ratios to produce combined feedstock biochars at different pyrolysis
104 temperatures to analyze the advantages, disadvantages, and application potential of the
105 produced biochars.

106 ## 2. Materials and methods

107 ### 2.1 Collection and preparation of raw materials

108 Japanese knotweed (*Fallopia japonica*) (JK) was harvested from Vlienderpad, a district in
109 Ghent, Belgium. The collected materials were washed with tap water three times to remove
110 external impurities. The solid fraction of pig manure (PM) was collected from the manure
111 treatment facility of IVACO, Gistel, Belgium, after on-site centrifuging to separate the thin
112 fraction from raw pig manure. The collected Japanese knotweed and pig manure were air-dried
113 for seven days, then oven-dried overnight at 75 °C to achieve constant weight. After that, the

materials were ground and sieved to 0.5 - 2 mm particles.

2.2 Biochar production

Ground PM and JK were mixed at mass ratios of 3:1, 1:1, and 1:3. PM without JK addition and JK without PM addition were used as controls. To produce different biochars, pure PM and JK and their mixtures were pyrolyzed at 400 °C, 500 °C, 600 °C, and 700 °C. This range of pyrolysis temperatures was chosen to cover the typical slow pyrolysis temperatures used for biochar production (Ronsse et al., 2013). All the experiments were performed in duplicate. Abbreviations for the biochars were composed of the symbol for the feedstocks, adding ratio, and temperature, e.g., P1J1-400 represents char produced by mixing PM and JK in a 1:1 mass ratio at 400 °C.

Fixed bed slow pyrolysis experiments were conducted with a modular stainless steel container, brought into a Carbolite Vertical Split Tube Furnace VST/TVS (Fig.1). The container tube with a diameter of 50 mm, and a height of 600 mm was filled with 100 g of feedstock; then, a split-tube furnace was used vertically to place the container (Fig.1). The furnace was connected to a nitrogen inlet at the bottom and an outlet line at the top for releasing produced gases and vapors, as shown in Fig. 1. By entering the reactor from below, nitrogen swept away the produced gases and vapors at a flow rate of 35 NL/h. Two sequential water-cooled spiral condensers allowed the gases and vapors produced during pyrolysis to condense completely. Round-bottom flasks were used to capture condensed vapors, while vents were used to vent the permanent gases. One thermocouple was used to measure the temperature at the center of the biomass bed beside the three built-in thermocouples needed for the three heating zones. After a transient heating-

up phase with an average heating rate of 15 °C/min, the reactor was held for an hour-long continuation at the chosen temperature (as measured by the thermocouple in the biochar bed). This residence time was selected based on previous works concerning char production from biomass and biochar stabilization by thermal treatment (Debela et al., 2012; Du et al., 2019). Once the holding period was over, the heater was turned off, the nitrogen flow was lowered to 6 NL/h, and the reactor tube was allowed to cool. After cooling down, the furnace was opened to retrieve the steel container with the chars and recover and weigh the generated biochars stored in airtight containers until further analysis. A summary of the operational parameters of the reactor is described in the Supplementary Material, Table S1.

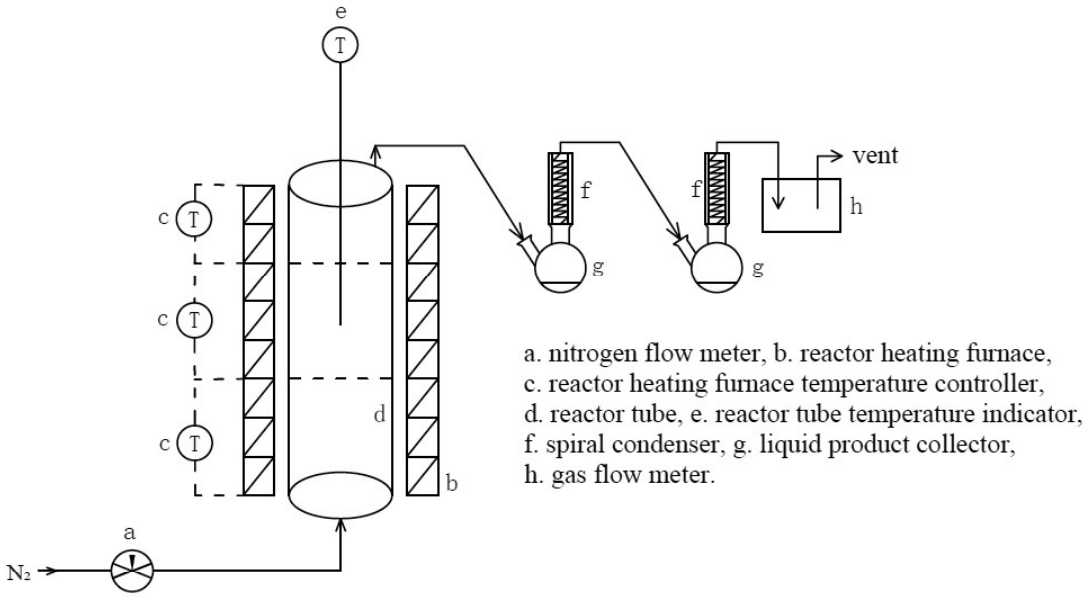

Fig.1. Scheme of the slow pyrolysis reactor

2.3 Biochar characterization

2.3.1 Yields calculation

The theoretical yield of combined feedstock biochar ($P1J1_{theoretical}$, $P1J3_{theoretical}$, and $P3J1_{theoretical}$) was calculated using Eq. 1 (Xu et al., 2019):

$$\mathrm{Yield_{theoretical}} = \mathrm{M} * \mathrm{Yield_{PM-T}} + (100 - \mathrm{M}) * \mathrm{Yield_{JK-T}} \quad \text{(Eq. 1)}$$

where $\mathrm{Yield_{PM\text{-}T}}$ (%) indicates the yield of pure PM-derived biochar at the given temperature T; $\mathrm{Yield_{JK\text{-}T}}$ (%) indicates the yield of pure JK-derived biochar at the given temperature T, and M (%) means the mass ratio of PM in the PM/JK mixture.

2.3.2 Biochar composition

As part of the proximate analysis, the ash content of feedstocks/biochar was calculated based on the mass percentage of residues after burning at 600 °C for 1 h in a muffle (Xue et al., 2019), and organic matter (OM) content was calculated by difference. With a muffle furnace heated at 500 °C for 1 h, volatile organic matter (VOM) content was determined by mass-loss rate. And according to the difference between OM and VOM, the fixed carbon content (FC) was estimated (Huang et al., 2017).

The ultimate elemental (C, H, N, and S) analysis of feedstocks/biochars was performed in an elemental analyzer (Thermo Fisher Scientific, Waltham, MA, USA), and the O content was calculated by difference.

For pH analysis, biochar was mixed with deionized water at a 1:20 (w:v) ratio, and the mixture was shaken for 1.5 hours to equilibrate the biochar-water solutions, then measured with a pH meter (Orion Star A211, Indonesia), following the TMECC methodology (International Biochar Initiative, 2015).

2.3.3 Heavy metals and nutrients analysis

For the determination of total heavy metals (HMs) and nutrients (Ca, K, Mg, and P), 0.5 g

feedstocks/biochars were digested with aqua regia at room temperature for 12 h followed by 2 h of digestion at boiling temperature (Van Ranst et al., 1999) and then the elemental contents were determined using inductively coupled plasma-optical emission spectrometry (ICP-OES; Varian Vista MPX, USA) (Wang et al., 2020b). Moreover, the residual rate (%) was adopted to evaluate the percentage of HMs and nutrients remaining in the biochar and was calculated following Eq. 2.

$$\text{Residual rate} = \frac{\text{Element}_{\text{biochar}}}{\text{Element}_{\text{feedstocks}}} \times \text{Yield} \quad \text{(Eq. 2)}$$

$CaCl_2$ solution for a single extraction was performed to simulate the environmental conditions associated with biochar utilization. 1 g of biochar samples were mixed with 20 mL of a 0.01 M $CaCl_2$ solution (solid: liquid = 1:20, w/v), and the mixture was shaken for 18 h at 200 rpm (Houba et al., 2000; Liu et al., 2019) at room temperature. After that, the mixtures were filtered, and the filtrates were analyzed by ICP-OES to determine their HM and nutrient contents.

The modified Community Bureau of Reference (BCR) sequential extraction procedure (von Gunten et al., 2017) was used to identify the chemical speciation of HMs in biochar. Heavy metals are classified into an acid/exchangeable fraction F1 (extracted with 0.1 M acetic acid), a reducible fraction F2 (0.1 M hydroxylammonium chloride, pH 2), an oxidizable fraction F3 (1.0 M ammonium acetate, pH 2), and a residual fraction F4 (aqua regia). The extracts were centrifuged at 4000 rpm for 20 min and filtered using a 0.45 μm membrane. The HMs concentrations of the extracts were analyzed using ICP-OES. The detailed extraction procedures are presented in Supplementary Material S1.

To evaluate the environmental risks of HMs in biochar, a potential environmental risk index

(RI) was calculated as follows (Du et al., 2019):

$$C_f = C_m / C_s \quad \text{(Eq. 3)}$$

$$E_r = T_f \times C_f \quad \text{(Eq. 4)}$$

$$RI = \sum E_r \quad \text{(Eq. 5)}$$

where C_f represents the individual heavy metal contamination factor; C_m and C_s represent the mobile fractions (F1+F2+F3) and the stable fraction (F4) of each heavy metal, respectively; T_f and E_r represent the toxic factor (1 for Zn and 5 for Cu) and the potential environmental risk for each metal, respectively (Du et al., 2019).

3. Results and discussion

3.1 Yield of biochar

To assess if co-pyrolysis of pig manure (PM) with Japanese knotweed (JK) would improve the yield and quality of the produced biochar, different mixing ratios and pyrolysis temperatures were tested, and the results are shown in Fig. 2. It is observed that biochar yields decreased with the increase in pyrolysis temperature (Fig. 2). A similar trend was also noticed for biochar derived from other feedstocks with increasing pyrolysis temperatures (Wang et al., 2021) and can be explained by extensive volatilization of the feedstocks, which cracks the biomass into pyrolytic gas and bio-oil, and further decomposition of the char at higher temperatures (Zhang et al., 2020).

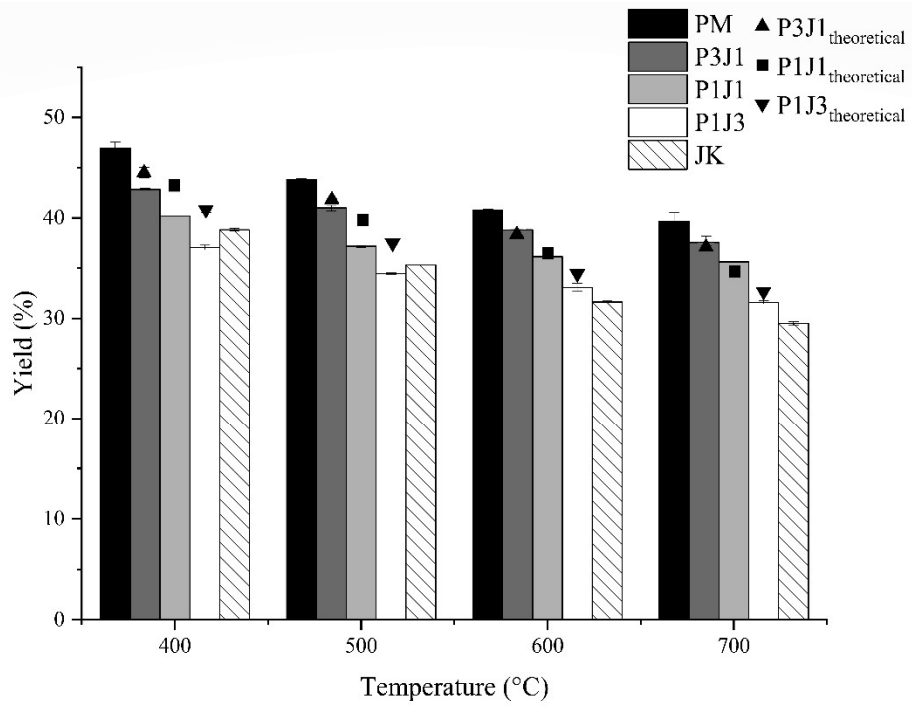

209

210 Fig. 2. The theoretical and experimental yields of biochar obtained at different pyrolysis
211 temperatures (P3J1, P1J1, and P1J3 indicate char produced by mixing PM with JK at 3:1, 1:1,
212 and 1:3 mass ratios)

213

214 Among all the produced materials, biochars derived from pure PM had the highest yield for
215 each temperature, while for JK, the opposite was true for the two highest temperatures. This
216 disparity could likely be ascribed to the higher ash content in PM (26.14%) than that in JK
217 (5.52%) since higher ash contents and lower organic content in the raw feedstock usually result
218 in a higher yield for the biochar produced at the same pyrolysis temperature (Xing et al., 2021).
219 As a result, the yields of the combined feedstock biochars were generally higher than that of
220 JK and lower than that of PM, decreasing with JK addition. An exception was observed for
221 P1J3 generated at 400 and 500 °C, which had slightly lower yields than the JK biochar produced
222 at the same temperature.

To gain an insight into the interaction between PM and JK and the reason for the exception mentioned above, the comparison between theoretical and experimental yields of the combined feedstock biochars is also shown in Fig. 2. During co-pyrolysis, the observed yields of combined feedstock biochars were lower than the theoretical values at lower pyrolysis temperatures (< 500 °C), indicating an antagonistic effect between PM and JK on solid-phase production. A possible explanation is the catalysis of organic constituents in the feedstock into volatiles by the presence of metals, i.e., the metals in the ash of PM possibly promoted secondary reactions such as cracking and dehydrogenation in the combined feedstock biochars, resulting in a reduced solid yield (Wang et al., 2016). This could also explain the lower char yield of P1J3-400 and P1J3-500 compared to JK-derived biochar. Increasing the temperature, however, reduced the difference between the theoretical and experimental values, suggesting that thermal cracking dominates over mineral-catalyzed cracking in such conditions.

3.2 Carbon-related characteristics of biochars

Table 1 shows the characteristics of PM, JK, and the produced biochars at different temperatures and mixing ratios. The pH values of the produced biochars increased with rising pyrolysis temperature compared to their respective feedstocks (Table 1), primarily due to the decomposition of acidic surface functional groups and the accumulation of alkali salts during pyrolysis (Cao and Harris, 2010). In addition, the heterocyclic groups (furans and others) can also take protons and act as basic groups during carbonation (Zhang et al., 2020). Among them, the pH of biochars prepared from JK varied the most, with a pH increase from 4.93 to 8.14 as pyrolysis temperatures increased from 400 °C to 700 °C, completely changing the original acidity. Compared with JK, PM-derived biochars showed a lower pH at the same pyrolysis

245 temperature, thus resulting in combined feedstock biochars with a lower pH than pure JK-
246 derived biochar. Meng et al. (2018) also noticed that rice straw-derived biochar held the highest
247 pH, while rice straw co-pyrolyzed with pig manure resulted in a more pronounced increase in
248 pH than pyrolysis manure alone. The high alkalinity of biochars has excellent potential for
249 ameliorating acidic soils and facilitating cationic immobilization (Tag et al., 2016).
250 Nevertheless, attention must be paid to avoid harming plant growth and soil quality when
251 adding such highly alkaline biochar, particularly in soil with low buffer capacity (Novak et al.,
252 2009).

253 The pyrolysis of PM and JK decreased the volatile organic matter (VOM) content and increased
254 the ash content in the derived biochars with rising temperatures (Table 1). It was also confirmed
255 that most VOM decomposed at 600 °C since no significant changes were recorded at a higher
256 temperature. PM and PM-derived biochars had the highest ash content, implying that most
257 inorganic constituents in PM concentrated and remained in the biochars after pyrolysis. The
258 addition of JK for co-pyrolysis of PM resulted in a decrease of approximately 30% (P1J1), 50%
259 (P1J3), and 15% (P3J1) of ash content in the combined feedstock biochars compared to PM-
260 derived biochars irrespective of the temperature. High ash content in biochar can improve soil
261 fertility by releasing inherent inorganic minerals; therefore, JK addition reduced such
262 micronutrient content that could benefit the soil. However, increasing mixing ratios of JK
263 resulted in higher fixed carbon (FC) contents in combined feedstock biochars, which have a
264 high potential for soil carbon storage. Co-pyrolysis of PM with JK increased nearly 1.5 folds
265 the FC contents in the combined feedstock biochars obtained at 600 °C compared with PM-
266 derived biochar. No further increase in FC content was observed when co-pyrolysis occurred

267 at a higher temperature (700 °C), which is similar to the result of Zhang et al. (2020), suggesting
268 that feedstock plays a primary role in influencing the FC content of the biochar and impacting
269 biochar carbon stability, not the temperature.

270 According to the ultimate elemental analysis of the produced biochar (Table 1), N, H, and O
271 contents decreased with increasing pyrolysis temperature, whereas C content increased. The
272 enrichment of C occurs through condensation and aromatization reactions, which involve the
273 processes of dehydration and dehydrogenation of the precursors, which are accompanied by
274 decarboxylation (Zhang et al., 2020); as the temperature rises, more H and O escape instead of
275 C. A reduction in nitrogen-containing compounds also accompanies these processes and finally
276 leads to the decrease of N (Jin et al., 2017). JK-derived biochars had the highest C contents;
277 therefore, the combined feedstock biochars with a higher JK addition correspondingly had a
278 higher C content. Such results suggested that organic compounds in the PM (mainly proteins,
279 sugars, lipids, and lipoids) are more unstable and thermally decompose more readily than JK
280 organic compounds (like cellulose, hemicellulose, and lignin). Furthermore, the C content did
281 not change significantly at the pyrolysis temperature higher than 600 °C, consistent with the
282 fixed carbon (FC) variation discussed earlier.

283 Ordinarily, H/C is used to evaluate the degree of aromatization in biochar and its stability
284 (Zhang et al., 2019), while O/C indicates its hydrophilicity and a higher degree of carbonization
285 (Karthik et al., 2021). The H/C of raw PM and JK were 2.03 and 1.54, and O/C ratios were 0.85
286 and 0.71, respectively. As the cracking reaction progressed, the molar H/C and O/C ratios of
287 the produced biochars decreased with the rising temperature (Supplementary Material, Fig. S1).

A further decrease in the H/C and O/C molar ratios of the combined feedstock biochars was observed with JK addition, indicating improved aromaticity and stability. Our study was consistent with previous findings on the decrease of the H/C of biochars resulting from the co-pyrolysis of rice husk or bamboo sawdust with sludge (Jin et al., 2017; Xu et al., 2019). The higher aromaticity of biochar is associated with its resistance to decomposition, reduced oxidation, and greater versatility as soil amendments (Huang et al., 2017). Schimelphfenning and Glaser (2012) studied the properties of biochar prepared from different raw materials under disparate reaction conditions and proposed that biochars with H/C < 0.6 and O/C < 0.4 are more suitable for soil improvement and carbon sequestration. Our study found that all generated combined feedstock biochars met these criteria (Supplementary Material, Fig. S1).

Table 1 Characteristics of pig manure (PM), Japanese knotweed (JK), and the produced biochars in dry basis (d.b.) at different pyrolysis temperatures (400, 500, 600, and 700 °C) and different mixing ratios (1:3, 1:1, and 3:1).

Samples	pH	Proximate analysis (wt% d.b.)			Ultimate analysis (wt% d.b.)			
		VOM	FC	Ash	C	H	N	O
JK	4.59±0.06	85.52±1.20	8.96±1.15	5.52±0.06	44.59±0.36	5.71±0.08	1.75±0.40	42.43±0.09
PM	7.39±0.05	69.86±0.30	4.01±0.13	26.14±0.44	30.97±1.51	5.23±0.14	2.51±0.14	35.15±1.08
JK-400	9.52±0.56	75.39±0.37	9.62±0.08	14.99±0.30	46.88±10.52	2.65±0.04	2.75±0.05	32.73±10.92
JK-500	10.04±0.01	68.04±0.21	15.99±0.42	15.97±0.64	68.72±0.84	1.16±0.21	1.89±0.19	12.26±1.87
JK-600	12.59±0.00	63.49±3.10	19.65±2.96	16.87±0.14	71.17±0.89	1.09±0.13	2.04±0.27	8.82±1.16
JK-700	12.73±0.01	62.75±1.46	19.97±1.54	17.29±0.08	73.58±0.13	0.82±0.04	2.02±0.13	6.29±0.12

PM-400	8.61±0.02	43.97±4.26	5.31±0.29	50.73±4.55	33.12±0.10	1.41±0.00	2.17±0.02	12.57±4.44
PM-500	9.81±0.01	39.23±1.51	8.75±1.50	56.03±0.01	36.24±2.70	1.22±0.32	1.84±0.01	8.68±3.00
PM-600	10.15±0.04	29.45±0.95	9.74±0.86	60.82±0.09	31.80±0.37	0.59±0.02	1.19±0.01	5.60±0.45
PM-700	10.46±0.08	28.81±0.68	9.22±0.13	61.97±0.55	34.72±2.23	0.41±0.01	0.87±0.02	2.03±1.70
P1J1-400	9.03±0.02	52.16±0.88	11.07±0.28	36.77±0.59	49.58±0.14	1.93±0.02	2.38±0.04	9.34±0.70
P1J1-500	9.25±0.01	47.75±1.14	13.03±0.05	39.23±1.09	53.74±1.58	1.41±0.05	2.22±0.08	3.40±0.45
P1J1-600	10.78±0.04	44.52±1.20	14.40±1.05	41.09±0.15	45.29±0.66	0.82±0.01	1.45±0.03	11.35±0.83
P1J1-700	11.77±0.16	42.14±0.08	14.32±2.44	43.55±2.52	48.27±2.80	0.54±0.01	1.27±0.04	6.38±5.36
P1J3-400	9.17±0.02	64.45±1.28	9.31±0.60	26.25±0.68	60.26±3.15	2.32±0.10	2.63±0.02	8.54±2.59
P1J3-500	9.59±0.00	59.53±0.73	14.88±2.33	25.60±1.60	60.14±1.22	1.53±0.05	2.22±0.03	10.50±2.91
P1J3-600	11.04±0.02	54.26±2.02	16.63±1.12	29.12±0.89	61.09±0.43	0.96±0.01	1.87±0.01	6.96±1.31
P1J3-700	11.91±0.02	53.24±0.18	17.60±0.04	29.17±0.14	62.54±1.42	0.70±0.08	1.51±0.05	6.08±1.40
P3J1-400	8.63±0.04	45.17±0.19	9.58±1.13	45.26±0.94	40.07±2.18	1.69±0.09	2.35±0.13	10.64±1.45
P3J1-500	8.76±0.01	38.51±1.81	13.83±1.52	47.67±0.29	44.12±1.85	1.19±0.10	2.15±0.16	4.88±1.82
P3J1-600	10.04±0.01	36.37±2.38	12.09±1.95	51.54±0.42	44.87±0.20	0.79±0.02	1.47±0.01	1.33±0.61
P3J1-700	11.29±0.08	34.71±3.01	12.37±2.75	52.93±0.26	44.66±0.75	0.62±0.13	1.07±0.02	0.72±0.37

3.3 Heavy metal composition of the produced biochars

3.3.1 Total HMs in the biochars

Fig. 3 shows the total Cu and Zn and the residual rate of these metals in the feedstocks and produced biochars. In terms of the total heavy metals in PM (Fig. 3), Zn (514 mg kg^{-1}) ranked first, followed by Cu (186 mg kg^{-1}). Other heavy metals like Ni, Cd, Cr, and Pb were below the detection limit in this study, even though these metals were reported by others working on

307 similar feedstocks (Lang et al., 2019; Wang et al., 2019). The high concentrations of metals in
308 manure could be ascribed to the extensive use of Cu and Zn supplements to promote pig growth
309 and prevent diarrhea (Yue et al., 2021). With rising pyrolysis temperature, the total Cu and Zn
310 in the PM-derived biochars gradually increased owing to the thermal decomposition of organic
311 matter in the feedstock (Xu et al., 2019). As expected, the total Cu (10 mg kg^{-1}) and Zn (31 mg
312 kg^{-1}) of JK were much lower than in PM. Accordingly, the total heavy metals in the combined
313 feedstock biochars with higher JK addition were lower than pyrolysis of PM alone at the same
314 temperature due to a dilution effect. However, as for the biochar yields, a small synergistic
315 effect was also observed for the Cu content of the co-pyrolysis biochars, with a measured Cu
316 content 5 - 16% lower than the content theoretically calculated. For Zn, this synergistic effect
317 was not observed, and in general, co-pyrolysis yields more or less the same measured content
318 for this metal as theoretically calculated.

319 To better understand the fate of Cu and Zn during pyrolysis, especially how much was
320 conserved in the biochar related to the initial content in the feedstocks, the residual rate was
321 calculated following Eq. 2. Fig. 3c shows that the Cu residual rates in all biochars exceeded
322 80%, indicating that this metal was mainly retained in the solid fraction due to its relatively low
323 vapor pressure and high boiling temperature of 1083.4 °C (Zeng et al., 2018). Zn residual rates,
324 however, were lower and decreased with temperature (Fig. 3d), showing less retention of Zn,
325 resulting in decreased Zn concentration in the generated biochars with increasing temperature.
326 The reason is attributed to the high volatility of Zn (boiling temperature of 419.5 °C) or the
327 formation of highly volatile metal chlorides (Xiao et al., 2015) that could easily promote the
328 volatilization of Zn into the gas stream when the temperature increases above 400 °C. To

329 prevent secondary pollution of the environment, it might be necessary to carefully collect and
330 treat the liquid and gas phases after co-pyrolysis.

331 Finally, to produce a qualified organic soil amendment, biochar should contain less than 300
332 mg kg^{-1} of dry matter of total Cu and less than 800 mg kg^{-1} of Zn, as recommended by the
333 European Union (EU, 2019). As expected, none of the PM-biochars met these limits in this
334 study due to the high Zn and Cu concentration in PM (Fig.3). However, the introduction of JK
335 to PM via co-pyrolysis beneficially reduced the total levels of heavy metals in the produced
336 biochars. P1J1 and P1J3 could meet the abovementioned requirements regardless of the
337 pyrolysis temperature.

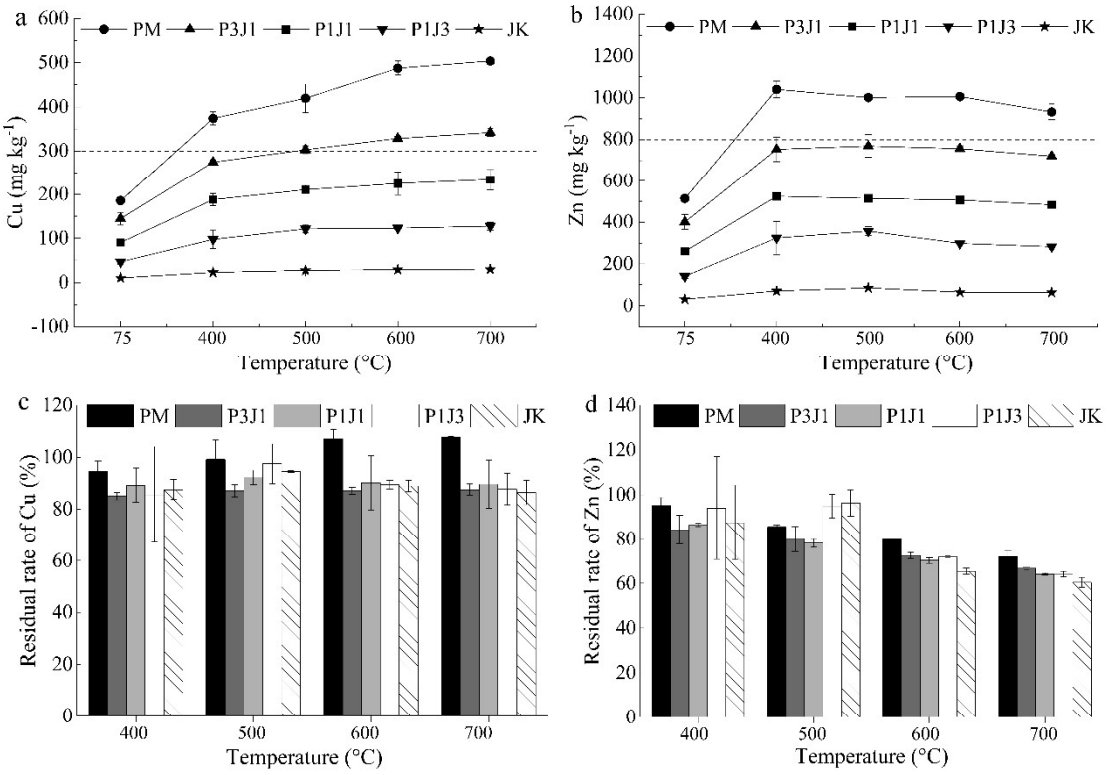

338

339 Fig. 3. Total concentrations of Cu (a) and Zn (b), and the residual rate of Cu (c) and Zn (d) in
340 feedstocks and biochars. 75°C is the temperature set to dry the feedstocks in the oven,
341 representing the temperature used for the analysis of raw materials; the dotted lines represent

342 the threshold of total Cu (less than 300 mg kg^{-1}) and Zn (less than 800 mg kg^{-1}) for soil
343 amendment required by EU

344 3.3.2 Speciation of HMs

345 Even though the combined feedstock biochars (P1J1 and P1J3) could meet the legal
346 requirements for total Cu and Zn contents, metal mobility is crucial to understanding their
347 potential environmental impact and toxicity. According to the BCR test, F1+F2 are the most
348 labile states, indicating high availability and direct eco-toxicity (Wang et al., 2021). F3 is
349 classified as a potentially effective state, relatively degradable under acidic and oxidizing
350 conditions. The stable F4 fraction keeps the metal within the crystal structure of primary and
351 secondary minerals (Du et al., 2019) and is less susceptible to dissolution. The differences in
352 distribution patterns of HMs are shown in Fig. 4.

353 For PM, over 70% of Zn was found in F1+F2, indicating an elevated environmental risk if PM
354 is directly applied to the soil. However, the proportion of Cu in PM of 90% in F3+F4 fractions
355 suggests that Cu predominated in the organic and residual fractions. When comparing the
356 fraction distributions of JK, F1+F2 of Zn (79.07%) and Cu (48.86%) were higher than those in
357 PM, indicating that JK also needs to be carefully processed to avoid possible environmental
358 risks by its direct use even though it has a much lower total metal content than PM.

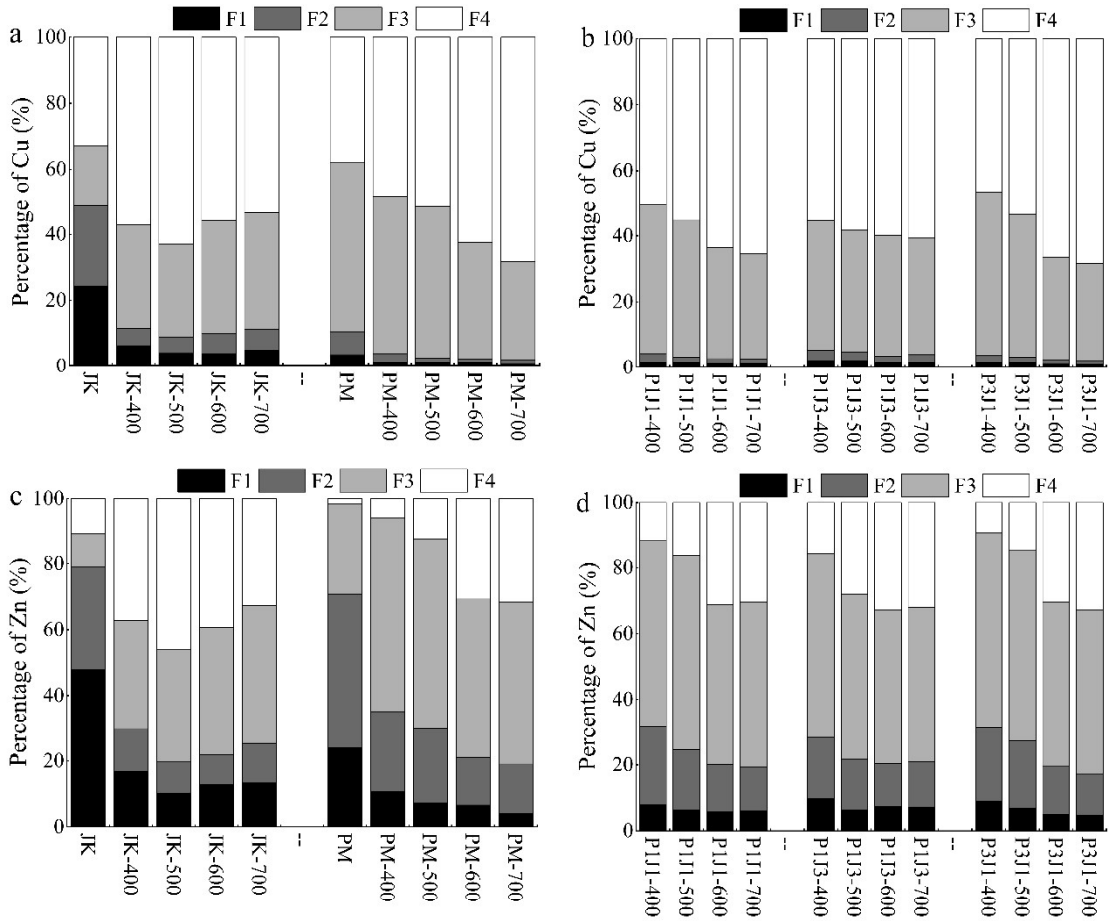

Fig. 4. Proportion changes in the speciation of Cu (a, b) and Zn (c, d) in feedstocks and biochars evaluated by the sequential extraction procedure following the BCR protocol. F1 is acid-soluble/exchangeable fraction, F2 is reducible fraction, F3 is oxidizable fraction, and F4 is residual fraction; and their availability and eco-toxicity decrease following the order: F1 > F2 > F3 > F4

When converting the feedstocks into biochar, the unstable portions (F1+F2) of Cu in PM were already lowered (3.74%) at 400 °C (Fig. 4a), which are then reduced to a lower valence and further to crystalline Cu with rising temperatures (Li et al., 2019), leading to oxidizable Cu (F3) transformed into the residual state (F4). The stable Cu (F4) in JK reached its highest value (63.03%) at 500 °C. Unstable Cu (F1+F2) in JK also decreased to the lowest value (8.90%) at

500 °C even though the found ratios were higher than those in PM (Fig. 4a). Consequently, F1+F2 Cu fractions in combined feedstock biochars were slightly higher after JK addition (Fig. 3b); nevertheless, JK addition did increase the stable Cu (F4) mainly due to its apparent increased F4 fraction at lower temperatures (≤ 500 °C). As the temperature rose to 600 °C and 700 °C, stable Cu increased at JK/PM ratios of 1:1 (P1J1) and 1:3 (P3J1) as more crystal Cu was formed with a higher PM addition.

Pyrolysis reduced the availability of Zn (F1+F2) in PM gradually to the lowest (19.04%) at 700 °C (Fig. 4c), and more stable Zn (F4) was also formed as the temperature rose, especially for temperatures higher than 600 °C (≥ 30.71%). The F1+F2 fractions of Zn in JK-derived biochars decreased to a minimum (19.85%), whereas the F4 fraction increased to a maximum (45.88%) at 500 °C. Thus, during the co-pyrolysis of PM with JK, the F1+F2 decrease and the F4 increase of Zn were more effective at higher JK addition and lower temperatures (≤ 500 °C). However, the increase in the JK ratio had a negligible effect on driving the decrease of F1+F2 and the rise of F4 at higher temperatures. In all the combined feedstock biochars, the non-available (F4) Zn increased to around 30% at 600 °C and 700 °C.

Based on the observed fractions of Cu and Zn in the resulting biochars, P1J1 prepared at 600 °C and 700 °C appears to result in a lower eco-toxicity (significant decline in the F1+F2 fraction) and higher stability (high formation of the F4 fraction) in the biochar. A high pyrolysis temperature, however, consumes more energy and produces less biochar. Additionally, Zn can volatilize into bio-oil and gases at a higher temperature, which may cause secondary pollution, as described before. Thus, 600 °C could be considered an optimum pyrolysis temperature

391 within the tested conditions since there is no significant difference between 600 °C and 700 °C.

392 ### 3.3.3 Bioavailability of HMs

393 To confirm the results obtained with the BCR procedure, $CaCl_2$-extraction was used to simulate
394 the actual environmental condition encountered in biochar utilization as a soil amendment (Du
395 et al., 2019) and correlated well with the Rhizon extractions and plant uptake (Van Poucke et
396 al., 2018) representing the direct bioavailability of HMs. The $CaCl_2$-extractable Cu and Zn are
397 shown in Fig. 5.

398 The values found were 4.27 and 34.44 mg kg^{-1} in PM and 2.51 and 3.99 mg kg^{-1} in JK for Cu
399 and Zn, respectively, and decreased when converting the feedstocks into biochars. $CaCl_2$-
400 extractable Cu and Zn in the JK-derived biochars achieved the lowest value at 500 °C, with the
401 extractable Cu increasing at higher temperatures. The bioavailable Cu in PM-derived biochars
402 also decreased and then slightly increased after 600 °C while Zn continuously decreased with
403 temperature. Increasing the temperature to certain degree results in the formation of exuberant
404 pores and stable aromatic structures in biochar, which can bind metal compounds to carbon
405 functional groups and reduce the amount of heavy metals that can be extracted (Du et al., 2019).
406 However, biochars pyrolyzed above a specific temperature tend to be more hydrophilic,
407 facilitating residual heavy metal leaching (Shen et al., 2020). The threshold temperature of this
408 study was 500 °C for JK and 600 °C for PM, and the difference might be attributed to the
409 organic and inorganic compositions difference between PM and JK, resulting in various
410 formations of organometallic or inorganic-metallic complexes during pyrolysis (Xu et al., 2019).
411 As a result, $CaCl_2$-extractable Cu and Zn in combined feedstock biochars decreased to the

lowest values in general at 600 °C and showed a no or slight increase after that. This result agreed with the changing behavior of F1+F2 fractions, further suggesting that 600 °C is enough to produce low bioavailability in the combined feedstock biochar, making it a better choice for co-pyrolysis of PM and JK.

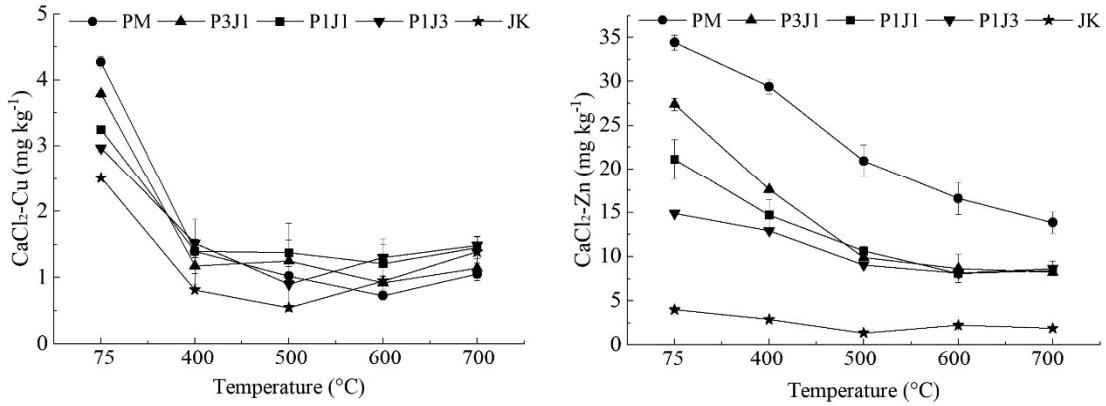

Fig. 5. Concentrations of $CaCl_2$-extracted Cu and Zn in feedstocks and biochars (75 °C is the temperature set to dry the feedstocks in the oven, representing the temperature used for the analysis of raw materials)

3.3.4 Environmental risk assessment

For further confirmation of the potential environmental risk of generated biochar by HMs, the contamination factor (C_f) and potential ecological risk (E_r) for each metal and the potential environmental risk index (RI value) were calculated and are shown in Table S2.

The C_f value of Cu in both PM and JK indicated low contamination, while, for Zn, this value indicated high contamination in PM and considerable contamination in JK. The E_r values for Zn demonstrated a moderate risk in PM and a low risk in JK. The RI value of PM suggested a moderate environmental risk when applied to soils and water, and Zn was the main contributor to this high RI (88.32%). Pyrolysis decreased the RI of PM, and the rising temperature further

enhanced this reduction, with all produced biochars having RI below the threshold value of 50, meaning low potential environmental risk.

In combined feedstock biochars, C_f, E_r, and RI decreased as JK/PM ratio increased, especially at 400 and 500 °C. Higher temperatures also reduced the RI to a great extent, but there was no significant difference between the different composite biochars. These results agree with the metal speciation analysis and further corroborate that P1J1 produced at 600 °C is a good combination for producing biochar with low contamination and potential environmental risk.

3.4 Nutrient content of biochars

Besides the changes in HMs, the inorganic minerals (P, Ca, K, and Mg) of feedstocks and pyrolysis-derived biochars are also worthy of attention and are shown in Fig. 6. PM was rich in Ca (23.80 mg kg^{-1}), Mg (24.34 mg kg^{-1}), and P (32.43 mg kg^{-1}), which was expected as PM has a high ash content and contains high amounts of inorganic minerals in its composition (Wang et al., 2020a). JK was rich in K (18.24 mg kg^{-1}), the most abundant cation in natural plants. Pyrolysis retained P, Ca, K, and Mg in biochars, as mineral alkali salts were released from the pyrolytic structure during the pyrolysis process. Similar results were reported for biochar produced from agricultural wastes and sludge (Karim et al., 2019; Rodriguez et al., 2021). As expected, co-pyrolysis of PM with JK resulted in a reduction of P, Ca, and Mg in combined feedstock biochars compared to the PM, but higher than those in JK, following the order: P3J1 > P1J1 > P1J3, consistent with the ash contents in the related biochars.

The average content of Ca, P, and Mg slightly decreased as the temperature increased from 600 to 700 °C, once more indicating that 600 °C was a better choice over 700 °C. In contrast, K

content increased as follows: JK > P1J3 > P1J1 > P3J1 > PM when the pyrolysis temperature increased. K in the plant reacts with the active functional groups produced from organic matter in cellulose during pyrolysis or intercalates in char layers to form insoluble char K and further transform into a more stable K_2CO_3 as temperature rises (Chen et al., 2017).

The accumulation of nutrients could be considered a bonus for the pyrolysis process. Rising the pyrolysis temperature can not only effectively reduce the bioactivity of heavy metals but also achieve nutrient retention. Among the three combined feedstock biochars, P1J1-600 preserved 70.16%, 55.00%, and 57.75% of Ca, Mg, and P, respectively, compared to PM-600, and 63.89% of K in contrast to JK-600. Taking P, Ca, Mg, and K into consideration also suggested that P1J1-600 would be a suitable candidate with a reasonable rate of nutrient conservation to produce the desired biochar.

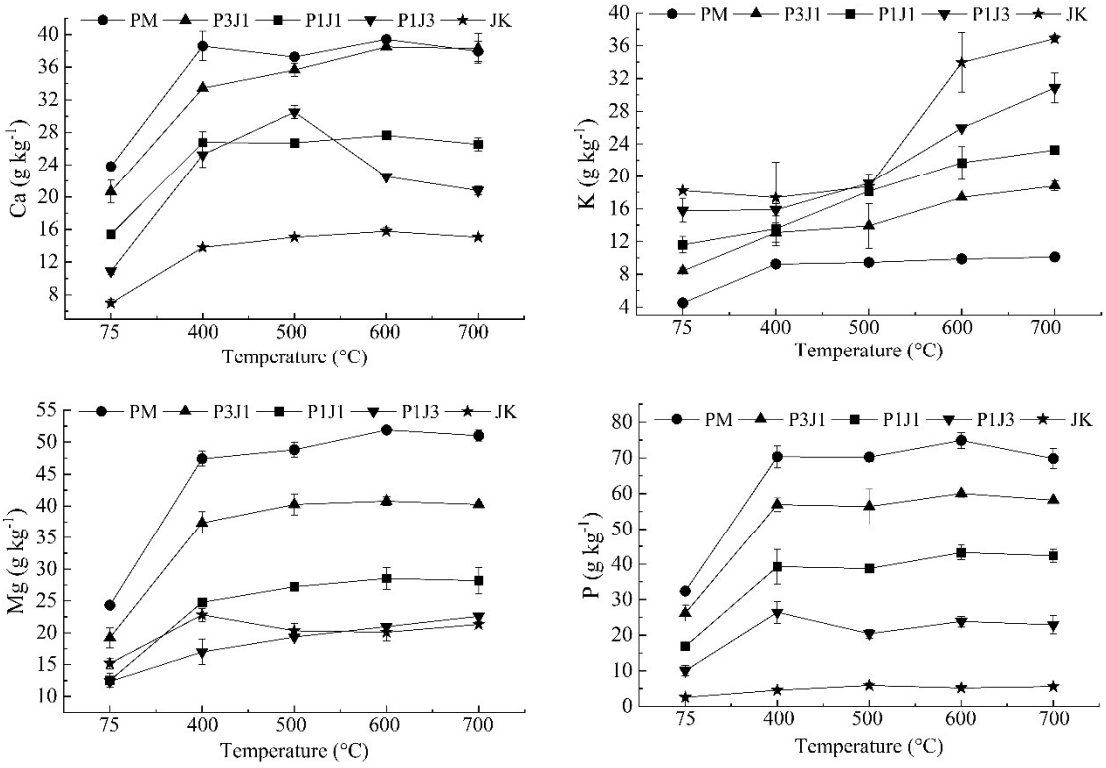

Fig. 6. Nutrient contents of feedstocks and biochars

463 Unlike the total nutrient concentration, the increase in pyrolysis temperature decreased the
464 bioavailable ($CaCl_2$-extractable) P, Ca, Mg, and K in the derived biochars of PM, JK, and their
465 mixtures to less than 2 g kg^{-1}, on average (Supplementary Material Fig. S2). As the temperature
466 increased, amorphous P, Ca, and Mg might have crystallized to form insoluble phosphate
467 minerals (calcium pyrophosphate and magnesium pyrophosphate), reducing the bioavailability
468 of P, Ca, and Mg in biochar (Rodriguez et al., 2021). The high total K also lays the foundation
469 for the higher bioavailable K in JK and derived biochar than other generated biochar;
470 nevertheless, the bioavailable K also decreased with increasing temperature. The low
471 extractable nutrients observed suggest that the generated biochars can act as a slow-release
472 nutrient source when applied to soils while limiting the leaching of excessive nutrients from
473 direct use.

474 Overall, when looking at biochar as an amendment for soil restoration, it is expected that the
475 final product would have high aromaticity, heavy metal presented in a stable form with low
476 bioavailability, low environmental risk, meet the total heavy metal control requirements of
477 organic soil improvers, and retain significant amounts of nutrients. The P1J1-600 biochar
478 obtained in this study met all of the abovementioned requirements and, therefore, can be
479 considered a suitable candidate for soil amendment. It is also worth noting that Cu and Zn,
480 highlighted in this study, are essential nutrients required in fertilizer programs for plant
481 production and development when present at relatively low concentrations. For the optimum
482 biochar P1J1-600 mentioned above, 46.16% of Cu and 50.38% of Zn were maintained in the
483 char compared with PM-600, reducing the total HMs concentration while effectively retaining
484 part of the Cu and Zn content to meet the total organic fertilizer requirement (Cu < 300 mg kg^{-}

485 [1], Zn < 800 mg kg^{-1}). In addition, the bioavailable proportion of Cu and Zn are also low when
486 looking at the most available fractions ($CaCl_2$-extractable, F1+F2) in P1J1-600, minimizing the
487 environmental risk while enabling the biochar to act as a nutrient source of these elements when
488 applied to soils.

489 ## 4. Conclusion

490 The co-pyrolysis of pig manure (PM) with Japanese knotweed (JK) was assessed to increase
491 the carbon content, reduce the metal content of pure PM-derived biochar, and enhance the
492 nutritional values of the plant-derived biochar. The combined feedstock biochar with half pig
493 manure and half Japanese knotweed addition prepared at 600 °C (P1J1-600) had the desired
494 properties with enhanced aromaticity, heavy metal presented in a more stable form with less
495 bioavailability, lowered environmental risk in terms of total heavy metal according to legal
496 requirements for organic improvers, and also retained the higher amount of nutrients, showing
497 great potential to be used as an amendment for soil restoration.

Reference

Ahmed, M. J., and Hameed, B. H. (2020). Insight into the co-pyrolysis of different blended feedstocks to biochar for the adsorption of organic and inorganic pollutants: A review. Journal of Cleaner Production 265, 121762.

Alfieri, A., and Mann, G. E. (2015). "Bioactive Nutraceuticals and Stroke," Bioactive Nutraceuticals and Dietary Supplements in Neurological and Brain Disease.

Cao, X., and Harris, W. (2010). Properties of dairy-manure-derived biochar pertinent to its potential use in remediation. Bioresource Technology 101, 5222-5228.

Chen, C., Luo, Z., Yu, C., Wang, T., and Zhang, H. (2017). Transformation behavior of potassium during pyrolysis of biomass. RSC Advances 7, 31319-31326.

Debela, F., Thring, R. W., and Arocena, J. M. (2012). Immobilization of Heavy Metals by Co-pyrolysis of Contaminated Soil with Woody Biomass. Water, Air, & Soil Pollution 223, 1161-1170.

Du, J., Zhang, L., Liu, T., Xiao, R., Li, R., Guo, D., Qiu, L., Yang, X., and Zhang, Z. (2019). Thermal conversion of a promising phytoremediation plant (Symphytum officinale L.) into biochar: Dynamic of potentially toxic elements and environmental acceptability assessment of the biochar. Bioresource Technology 274, 73-82.

EU, R. (2019). Regulation (EU) 2019/1009 of the European Parliament and of the Council of 5 June 2019 laying down rules on the making available on the market of EU fertilising products and amending Regulations (EC) No 1069/2009 and (EC) No 1107/2009 and repealing Regulation (EC) No 2003/2003. Offi. J. Eur. Union 62, 1-114.

Feng, Q., Wang, B., Chen, M., Wu, P., Lee, X., and Xing, Y. (2021). Invasive plants as potential sustainable feedstocks for biochar production and multiple applications: A review. Resources, Conservation and Recycling 164, 105204.

521 Gao, R., Hu, H., Fu, Q., Li, Z., Xing, Z., Ali, U., Zhu, J., and Liu, Y. (2020). Remediation of Pb, Cd, and
522 Cu contaminated soil by co-pyrolysis biochar derived from rape straw and orthophosphate:
523 Speciation transformation, risk evaluation and mechanism inquiry. Science of The Total
524 Environment 730, 139119.
525 Garlapalli, R. K., Wirth, B., and Reza, M. T. (2016). Pyrolysis of hydrochar from digestate: Effect of
526 hydrothermal carbonization and pyrolysis temperatures on pyrochar formation. Bioresource
527 Technology 220, 168-174.
528 Ghysels, S., Acosta, N., Estrada, A., Pala, M., De Vrieze, J., Ronsse, F., and Rabaey, K. (2020).
529 Integrating anaerobic digestion and slow pyrolysis improves the product portfolio of a cocoa
530 waste biorefinery. Sustainable Energy & Fuels 4, 3712-3725.
531 Houba, V. J. G., Temminghoff, E. J. M., Gaikhorst, G. A., and van Vark, W. (2000). Soil analysis
532 procedures using 0.01 M calcium chloride as extraction reagent. Communications in Soil
533 Science and Plant Analysis 31, 1299-1396.
534 Huang, H.-j., Yang, T., Lai, F.-y., and Wu, G.-q. (2017). Co-pyrolysis of sewage sludge and sawdust/rice
535 straw for the production of biochar. Journal of Analytical and Applied Pyrolysis 125, 61-68.
536 International Biochar Initiative (2015). Standardized product definition and product testing guidelines
537 for biochar that is used in soil. Int. Biochar Initiat 23.
538 Jiang, B., Lin, Y., and Mbog, J. C. (2018). Biochar derived from swine manure digestate and applied on
539 the removals of heavy metals and antibiotics. Bioresource Technology 270, 603-611.
540 Jin, J., Wang, M., Cao, Y., Wu, S., Liang, P., Li, Y., Zhang, J., Zhang, J., Wong, M. H., Shan, S., and
541 Christie, P. (2017). Cumulative effects of bamboo sawdust addition on pyrolysis of sewage
542 sludge: Biochar properties and environmental risk from metals. Bioresource Technology 228,

218-226.

Kameyama, K., Miyamoto, T., and Iwata, Y. (2020). Comparison of plant Cd accumulation from a Cd-contaminated soil amended with biochar produced from various feedstocks. Environmental Science and Pollution Research, 1-8.

Karim, A. A., Kumar, M., Mohapatra, S., and Singh, S. K. (2019). Nutrient rich biomass and effluent sludge wastes co-utilization for production of biochar fertilizer through different thermal treatments. Journal of Cleaner Production 228, 570-579.

Karthik, V., Kumar, P. S., Vo, D.-V. N., Sindhu, J., Sneka, D., Subhashini, B., Saravanan, K., and Jeyanthi, J. (2021). Hydrothermal production of algal biochar for environmental and fertilizer applications: a review. Environmental Chemistry Letters 19, 1025-1042.

Köninger, J., Lugato, E., Panagos, P., Kochupillai, M., Orgiazzi, A., and Briones, M. J. I. (2021). Manure management and soil biodiversity: Towards more sustainable food systems in the EU. In "Agricultural Systems", Vol. 194, pp. 103251.

Lang, Q., Chen, M., Guo, Y., Liu, Z., and Gai, C. (2019). Effect of hydrothermal carbonization on heavy metals in swine manure: Speciation, bioavailability and environmental risk. Journal of Environmental Management 234, 97-103.

Li, H., Hu, J., Yao, L., Shen, Q., An, L., and Wang, X. (2020). Ultrahigh adsorbability towards different antibiotic residues on fore-modified self-functionalized biochar: Competitive adsorption and mechanism studies. Journal of Hazardous Materials 390, 122127.

Li, R., Huang, H., Wang, J. J., Liang, W., Gao, P., Zhang, Z., Xiao, R., Zhou, B., and Zhang, X. (2019). Conversion of Cu(II)-polluted biomass into an environmentally benign Cu nanoparticles-embedded biochar composite and its potential use on cyanobacteria inhibition. Journal of

565 Cleaner Production 216, 25-32.
566 Liu, C.-H., Chu, W., Li, H., Boyd, S. A., Teppen, B. J., Mao, J., Lehmann, J., and Zhang, W. (2019).
567 Quantification and characterization of dissolved organic carbon from biochars. Geoderma 335,
568 161-169.
569 Makara, A., and Kowalski, Z. (2018). Selection of pig manure management strategies: Case study of
570 Polish farms. Journal of Cleaner Production 172, 187-195.
571 Mendonça, F. G. d., Cunha, I. T. d., Soares, R. R., Tristão, J. C., and Lago, R. M. (2017). Tuning the
572 surface properties of biochar by thermal treatment. Bioresource Technology 246, 28-33.
573 Meng, J., Liang, S., Tao, M., Liu, X., Brookes, P. C., and Xu, J. (2018). Chemical speciation and risk
574 assessment of Cu and Zn in biochars derived from co-pyrolysis of pig manure with rice straw.
575 Chemosphere 200, 344-350.
576 Novak, J. M., Busscher, W. J., Laird, D. L., Ahmedna, M., Watts, D. W., and Niandou, M. A. S. (2009).
577 Impact of Biochar Amendment on Fertility of a Southeastern Coastal Plain Soil. Soil Science
578 174, 105-112.
579 Rodriguez, J. A., Lustosa Filho, J. F., Melo, L. C. A., de Assis, I. R., and de Oliveira, T. S. (2021). Co-
580 pyrolysis of agricultural and industrial wastes changes the composition and stability of biochars
581 and can improve their agricultural and environmental benefits. Journal of Analytical and
582 Applied Pyrolysis 155, 105036.
583 Ronsse, F., Van Hecke, S., Dickinson, D., and Prins, W. (2013). Production and characterization of slow
584 pyrolysis biochar: influence of feedstock type and pyrolysis conditions. Gcb Bioenergy 5, 104-
585 115.
586 Shen, X., Zeng, J., Zhang, D., Wang, F., Li, Y., and Yi, W. (2020). Effect of pyrolysis temperature on

587 characteristics, chemical speciation and environmental risk of Cr, Mn, Cu, and Zn in biochars
588 derived from pig manure. The Science of the Total Environment 704, 135283.1-135283.11.
589 Tag, A. T., Duman, G., Ucar, S., and Yanik, J. (2016). Effects of feedstock type and pyrolysis temperature
590 on potential applications of biochar. Journal of Analytical and Applied Pyrolysis 120, 200-206.
591 Van Poucke, R., Ainsworth, J., Maeseele, M., Ok, Y. S., Meers, E., and Tack, F. M. G. (2018). Chemical
592 stabilization of Cd-contaminated soil using biochar. Applied Geochemistry 88, 122-130.
593 Van Ranst, E., Verloo, M., Demeyer, A., and Pauwels, J. (1999). "Manual for the soil chemistry and
594 fertility laboratory: analytical methods for soils and plants equipment, and management of
595 consumables."
596 von Gunten, K., Alam, M. S., Hubmann, M., Ok, Y. S., Konhauser, K. O., and Alessi, D. S. (2017).
597 Modified sequential extraction for biochar and petroleum coke: Metal release potential and its
598 environmental implications. Bioresource Technology 236, 106-110.
599 Wang, A., Zou, D., Zhang, L., Zeng, X., Wang, H., Li, L., Liu, F., Ren, B., and Xiao, Z. (2019).
600 Environmental risk assessment in livestock manure derived biochars. RSC Advances 9, 40536-
601 40545.
602 Wang, K., Peng, N., Lu, G., and Dang, Z. (2020a). Effects of Pyrolysis Temperature and Holding Time
603 on Physicochemical Properties of Swine-Manure-Derived Biochar. Waste and Biomass
604 Valorization 11, 613-624.
605 Wang, X., Chang, W. C., Li, Z., Chen, Z., and Wang, Y. (2021). Co-pyrolysis of sewage sludge and
606 organic fractions of municipal solid waste: Synergistic effects on biochar properties and the
607 environmental risk of heavy metals. Journal of Hazardous Materials 412, 125200.
608 Wang, X., Deng, S., Tan, H., Adeosun, A., Vujanović, M., Yang, F., and Duić, N. (2016). Synergetic

609 effect of sewage sludge and biomass co-pyrolysis: A combined study in thermogravimetric
610 analyzer and a fixed bed reactor. Energy Conversion and Management 118, 399-405.
611 Wang, X., Fernandes de Souza, M., Li, H., Tack, F. M. G., Ok, Y. S., and Meers, E. (2020b). Zn
612 phytoextraction and recycling of alfalfa biomass as potential Zn-biofortified feed crop. Sci Total
613 Environ, 143424.
614 Xiao, Z., Yuan, X., Li, H., Jiang, L., Leng, L., Chen, X., Zeng, G., Li, F., and Cao, L. (2015). Chemical
615 speciation, mobility and phyto-accessibility of heavy metals in fly ash and slag from combustion
616 of pelletized municipal sewage sludge. Science of The Total Environment 536, 774-783.
617 Xing, J., Xu, G., and Li, G. (2021). Comparison of pyrolysis process, various fractions and potential soil
618 applications between sewage sludge-based biochars and lignocellulose-based biochars.
619 Ecotoxicology and Environmental Safety 208, 111756.
620 Xu, Y., Qi, F., Bai, T., Yan, Y., Wu, C., An, Z., Luo, S., Huang, Z., and Xie, P. (2019). A further inquiry
621 into co-pyrolysis of straws with manures for heavy metal immobilization in manure-derived
622 biochars. Journal of Hazardous Materials 380, 120870.
623 Xue, Y., Wang, C., Hu, Z., Zhou, Y., Xiao, Y., and Wang, T. (2019). Pyrolysis of sewage sludge by
624 electromagnetic induction: Biochar properties and application in adsorption removal of Pb(II),
625 Cd(II) from aqueous solution. Waste Management 89, 48-56.
626 Yue, Z., Zhang, J., Zhou, Z., Ding, C., Wan, L., Liu, J., Chen, L., and Wang, X. (2021). Pollution
627 characteristics of livestock faeces and the key driver of the spread of antibiotic resistance genes.
628 Journal of Hazardous Materials 409, 124957.
629 Zeng, X., Xiao, Z., Zhang, G., Wang, A., Li, Z., Liu, Y., Wang, H., Zeng, Q., Liang, Y., and Zou, D.
630 (2018). Speciation and bioavailability of heavy metals in pyrolytic biochar of swine and goat

manures. Journal of Analytical and Applied Pyrolysis 132, 82-93.

Zhang, J., Jin, J., Wang, M., Naidu, R., and Shan, S. (2020). Co-pyrolysis of sewage sludge and rice husk/ bamboo sawdust for biochar with high aromaticity and low metal mobility. Environmental Research, 110034.

Zhang, Y., Jiang, Q., Xie, W., Wang, Y., and Kang, J. (2019). Effects of temperature, time and acidity of hydrothermal carbonization on the hydrochar properties and nitrogen recovery from corn stover. Biomass and Bioenergy 122, 175-182.